COBEM 2021 26th International Congress of Mechanical Engineering
November 22-26, 2021, Virtual Congress, Brazil
ABCM Associação Brasileira de Engenharia e Ciências Mecânicas

COB-2021-0291
GENERATION OF NARROW-BAND *C*-DISTRIBUTIONS FOR THE BANDED-SLW MODEL

Guilherme Crivelli Fraga
Felipe Ramos Coelho
Francis Henrique Ramos França
Federal University of Rio Grande do Sul, Mechanical Engineering Department - 425 Sarmento Leite St., Porto Alegre, RS Brazil
guilhermecfraga@gmail.com
f.ramoscoelho@gmail.com
frfranca@mecanica.ufrgs.br

Abstract. *Narrow-band C-distributions are generated for water vapor and carbon dioxide using absorption spectra extracted from the high-resolution spectroscopic database HITEMP2010, for conditions typically found in atmospheric combustion processes. These C-distributions are similar to the k-distributions used in some narrow-band models, but they are set up in a more convenient way for utilization with the spectral line-based weighted-sum-of-gray-gases (SLW) and banded-SLW models. Narrow-band mean absorption coefficients and emittances calculated from the C-distributions show remarkable agreement with data computed directly from the high-resolution spectra (errors of less than* 0.1 %*), and both full-spectrum and partial-spectrum absorption line blackbody distribution functions (ALBDFs) can be assembled from the narrow-band distributions with a high degree of accuracy. Finally, a sample of cases consisting of non-coupled, one-dimensional radiative heat transfer calculations are tested to illustrate how the C-distributions obtained here can be applied to the SLW and banded-SLW models.*

Keywords: *Thermal radiation, spectral modeling, narrow-band k-distributions, high-resolution absorption spectra, SLW model*

1. INTRODUCTION

Line-by-line (LBL) integration can predict the radiative transfer in participating gaseous media with a high-degree of accuracy, but the exceedingly large computational cost of this method makes it unpractical for most engineering applications (Howell *et al.*, 2016). For small spectral intervals, within which the Planck function and other radiative properties can be regarded as approximately constant, the highly oscillating gas spectral absorption coefficient κ_η assumes the same value k multiple of times. This observation has led to the proposal of a reordering of κ_η into a smooth, monotonically increasing function, which can be more efficiently integrated over the wavenumber spectrum η. This approach is known as the narrow-band k-distribution model (Lacis and Oinas, 1991; Goody and Yung, 1995), and, while essentially exact for homogeneous media, application of the model to non-homogeneous conditions is challenging and requires the introduction of additional assumptions (Modest, 2013).

The concept of reordering of the absorption coefficient can also be applied to the entire radiation spectrum. This is the basis of the full-spectrum k-distribution (FSK) (Modest and Zhang, 2002) and of the spectral line-based weighted-sum-of-gray-gases (SLW) models (Denison and Webb, 1993b), although in the case of the latter the reordering is made in terms of the spectral absorption cross-section C_η rather than κ_η. Since their proposal, both of these models have shown to provide a good compromise between accuracy and computational efficiency for a wide variety of problems (Modest, 2013; Webb *et al.*, 2019). However, because information on the spectral dependence of the absorption coefficient is completely lost in the reordering of κ_η across the full spectrum, the FSK and SLW models are not capable of accommodating non-gray scattering particles or non-gray wall reflectivities.

A promising approach, that combines the accuracy and versatility of the FSK and SLW models while still being able to solve these more difficult types of problems, is to carry out the κ_η or C_η reordering successively over wide portions of the spectrum into which the non-gray scattering or reflectivities can be taken as constant. This method was fist proposed by Denison and Webb, 1994, in the framework of the SLW model, and afterwards extended by Modest and Riazzi, 2005, to the FSK model. More recently, this idea has regained popularity with a series of works by the research group of Selçuk and Kulah (Ozen *et al.*, 2019; Yasar *et al.*, 2020a,b, 2021a,b), where the method was referred to as the banded-SLW model and was successfully applied to a series of problems involving fluidized-bed combustion. A limitation of those studies, however, is that they all rely on narrow-band k-distributions generated by Denison, 1994, that, besides considering fairly large narrow-bands, were developed on the basis of out-of-date spectral data.

In light of this, the present paper aims to obtain new narrow-band C-distributions based on the up-to-date, high-resolution spectroscopic database HITEMP2010 (Rothman *et al.*, 2010). These distributions are generated for CO_2 and H_2O, two of the most important participating species produced by common combustion processes, at atmospheric pressure and for temperatures ranging between 300 K and 2500 K. While similar work has been carried out for narrow-band k-distributions (the most recent example being Cai and Modest, 2014), no previous author reports databases conveniently set up for utilization with the SLW or banded-SLW models. Furthermore, as it will be shown, the data set with the new narrow-band C-distributions developed here requires much less storage space than the corresponding k-distributions of Cai and Modest, 2014.

2. RADIATIVE TRANSFER AND THE BANDED-SLW MODEL

The spectral radiative intensity I_η traveling along an optical path s can be determined from the solution of the radiative transfer equation (RTE). Assuming a non-scattering medium, the RTE yields (Modest, 2013)

$$\frac{\mathrm{d}I_\eta}{\mathrm{d}s} = \kappa_\eta \left(I_{b\eta} - I_\eta\right), \tag{1}$$

where $I_{b\eta}$ is the blackbody spectral intensity and κ_η is the spectral absorption coefficient of the medium. For a gaseous mixture of typical combustion products, such as carbon dioxide and water vapor, κ_η exhibits a highly irregular dependence on the wavenumber η, characterized by hundreds of thousands to million of absorption lines whose position may also depend on the local medium temperature T_g, pressure p and mole fraction X.

To determine the total radiative intensity $I = \int_0^\infty I_\eta \,\mathrm{d}\eta$, Eq. (1) must be solved for each one of these lines individually. Because such task can be very computationally intensive, this led to the development of a number of spectral models. Of interest to this paper are global or full-spectrum models, that solve the RTE after it is integrated over a series of non-contiguous portions $\Delta\eta_j$ of the spectrum, each of which having a constant (with respect to η) absorption coefficient κ_j (Howell *et al.*, 2016). These portions are conventionally called gray gases, and for each one j the RTE is written as (Modest, 1991; Webb *et al.*, 2019)

$$\frac{\mathrm{d}I_j}{\mathrm{d}s} = \kappa_j \left(w_j I_b - I_j\right), \tag{2}$$

which is obtained by integrating Eq. (1) over $\Delta\eta_j$. In the above equation, I_j is the partial radiative intensity corresponding to gas j, strictly defined as $I_j = \int_{\Delta\eta_j} I_\eta \,\mathrm{d}\eta$; $I_b = \int_0^\infty I_{b\eta} \,\mathrm{d}\eta$ is the total blackbody intensity; and w_j is an emission-weighting function that quantifies the fraction of blackbody energy that lies within $\Delta\eta_j$, or $w_j = \int_{\Delta\eta_j} I_{b\eta} \,\mathrm{d}\eta \,/ I_b$. Once Eq. (2) has been solved for the total number of J non-contiguous portions of the spectrum, the total intensity is then obtained as $I = \sum_{j=0}^{J} I_j$ (where $j = 0$ indicates the transparent portions of the spectrum, with $\kappa_0 = 0$ and $w_0 = 1 - \sum_{j=1}^{J} w_j$).

The various full-spectrum models available in the literature differ from one another in how the size and location of the spectral portions $\Delta\eta_j$ are defined, and in the manner in which the κ_j and w_j parameters are computed. In this paper, only the spectral line-based weighted-sum-of-gray-gases (SLW) model is described in details, since it is the basis for the banded model that motivates the generation of the narrow-band C-distributions reported in the present study.

2.1 The absorption line blackbody distribution function and the SLW model

The absorption line blackbody distribution function (ALBDF) was introduced by Denison and Webb, 1993a, as a way to conveniently compute the spectral integration required to evaluate the weighting coefficient w_j. For historical reasons, this function is expressed in terms of the spectral absorption cross-section, C_η, rather than the spectral absorption coefficient κ_η. Nevertheless, the two quantities can be related as (Solovjov *et al.*, 2018)

$$\kappa_\eta(\phi) = NXC_\eta(\phi), \tag{3}$$

where N is the gas molar density (a known function of the gas temperature and total pressure), and the dependence of both κ_η and C_η on the thermodynamic state ϕ is denoted explicitly—here, ϕ symbolically represents the thermodynamic state, $\phi = \{T_g, X, p\}$, and it will be useful to keep this dependence explicit in the discussions to come.

In this framework, the ALBDF F is defined as the fraction of the blackbody energy at a given source temperature T_b that lies within the wavenumber intervals for which the absorption cross-section $C_\eta(\phi)$ of a medium at thermodynamic state ϕ is below a prescribed value C. Mathematically, this can be expressed as (Webb *et al.*, 2019)

$$F(C, \phi, T_b) = \int_0^\infty H\left[C - C_\eta(\phi)\right] \frac{I_{b\eta}(T_b)}{I_b(T_b)} \,\mathrm{d}\eta \,, \tag{4}$$

in which $H[x]$ is the Heaviside step function, $I_{b\eta}(T_b)$ and $I_b(T_b)$ are the spectral and total blackbody intensities evaluated at T_b, respectively, and all dependences of F are also indicated explicitly.

Equation (4) is the basis for the construction of the SLW model (Denison and Webb, 1993b). The main conceit of this model is as follows: first, the continuous absorption cross-section variable C is discretized into supplemental cross-sections $\tilde{C}_j$ (with $j = 0, 1, \ldots, J$), whose values are defined as to encompass the full range of the C_η spectrum, and which are usually distributed in a logarithm fashion. Then, for any given $0 < j \leq J$, the weighting function w_j is given as $w_j = F(\tilde{C}_j, \phi, T_b) - F(\tilde{C}_{j-1}, \phi, T_b)$; for $j = 0$, that again denotes the transparent portions of the spectrum, $w_j = F(\tilde{C}_0, \phi, T_b)$. Finally, to determine the absorption cross-section value C_j of each gas j—from whence κ_j can be computed, following Eq. (3)—the traditional approach has been to take a geometric mean of the supplemental absorption cross-sections, $C_j = \sqrt{\tilde{C}_j \tilde{C}_{j+1}}$ (except for $j = 0$, where, by definition, $C_0 = 0$). In this manner, both κ_j and w_j can be determined for each j, from which Eq. (2) can be solved, and, ultimately, the total radiative intensity is obtained.

Notice that the procedure described in the previous paragraph is only strictly valid for uniform media. If the thermodynamic state of the medium varies along the optical path, the boundaries of the spectral portions j used for the integration of the RTE from Eq. (1) to Eq. (2) can vary with s, which leads to the appearance of Leibnitz terms, that, if neglected, can yield significant errors in the prediction of the radiation field (Webb *et al.*, 2019). To avoid this issue, the SLW model aims to maintain the boundaries of the spectral portions constant throughout the optical path by introducing a reference state, from which the local supplemental cross-sections are defined in a way that the spectral regions $\Delta\eta_j$ do not change with the location. There are many different approaches for achieving this, whose underlying assumptions and details are outside the scope of the present paper; the interested reader is referred to a thorough review of the SLW model presented by Webb *et al.*, 2019.

2.2 The banded-SLW model

The standard SLW model has, like any full-spectrum model, some important limitations inherent to its formulation. The integration of the RTE over the entire spectrum that yields Eq. (2) leads to a loss of information regarding the absorption spectrum of the medium. This makes the treatment of non-gray boundaries and particulate with non-gray scattering properties challenging, requiring additional assumptions and models.

A fairly simple, promising approach for these types of problems is the banded SLW model. This approach was introduced by Denison and Webb, 1994, as a hybrid method, combining features of the WSGG model and the k-distribution method as a way to accommodate non-gray boundaries and scattering in the framework of full-spectrum models. A similar formulation was later proposed by Modest and Riazzi, 2005, in the framework the FSK model, also with the purpose of extending the model to the aforementioned conditions. More recently, this hybrid method was applied by Kulah's group (Ozen *et al.*, 2019; Yasar *et al.*, 2020a,b, 2021a,b) to many problems involving fluidized-bed combustion; in these last set of references, the method was named the banded-SLW (BSLW) model, since, to find the parameters of each gray gas within each band, the cumulative k-distribution function was used in a similar manner as to how the ALBDF is employed to find κ_j and w_j in the standard SLW model. A discussion on k-distributions and how they can be used to assemble the parameters of the BSLW model is left to Section 3; here, only the main formulation of the banded SLW model is presented.

In the BSLW model, the absorption spectrum of the medium is divided into M contiguous bands, within each of which the standard formulation of the SLW model is applied—the difference being that the banded SLW model parameters are not defined in terms of the full wavenumber spectrum, but rather on the spectral interval corresponding to the band. The position and size of the bands is arbitrary, and is usually defined as to match a stepwise representation of the non-gray spectral emissivities of the boundaries or of the non-gray scattering coefficient and phase function. Following this formulation, for an arbitrary band m, the RTE for gas j becomes

$$\frac{\mathrm{d}I_{j,m}}{\mathrm{d}s} = \kappa_{j,m}\left(w_{j,m} I_b - I_{j,m}\right), \tag{5}$$

with the total radiative intensity now given as a double summation over all M bands and all J_m gray gases (where the latter can be different from band to band), $I = \sum_{m=1}^{M} \sum_{j=0}^{J_m} I_{j,m}$.

In Eq. (5), the absorption coefficient of each gray gas within each band, $\kappa_{j,m}$, can be computed in the same manner as in the full-spectrum SLW model described in Section 2.1—i.e., from the supplemental absorption cross-sections $\tilde{C}_{j,m}$ and $\tilde{C}_{j+1,m}$, although in the BSLW model the positions of these cross-sections can differ from band to band. On the other hand, the weighting coefficient $w_{j,m}$ needs to be evaluated taking into consideration only the spectral interval corresponding to band m: $w_{j,m} = \int_{\Delta\eta_{j,m}} I_{b\eta}\,\mathrm{d}\eta \,/ I_b$, where $\Delta\eta_{j,m}$ represents the (non-contiguous) portion of the radiation spectrum occupied by gas j within band m. To evaluate this quantity, one needs an ALBDF-like function that, rather than the full spectrum (as in Eq. (4)), is computed over band m alone. This function, named here the partial ALBDF, can be defined as

$$F_{\Delta\eta_m}(C, \phi, T_b) = \int_{\eta_{m-1}}^{\eta_m} H\left[C - C_\eta(\phi)\right] \frac{I_{b\eta}(T_b)}{I_b(T_b)} \mathrm{d}\eta, \tag{6}$$

in which η_{m-1} and η_m are the lower and upper bounds that characterize the band, respectively.

In principle, Eq. (6) could be directly calculated from the absorption spectrum of the medium and then tabulated in terms of C, ϕ and T_b in a similar manner as the full-spectrum ALBDF has been (see, for instance, Pearson *et al.*, 2014). However, this is not practical, because one would need to produce tables for a large number of η_m and η_{m+1} combinations, since the position and size of the bands into which the medium is divided depends on the modeling choices and on the specific problem under investigation. A more sensible approach, therefore, is to compute Eq. (6) from narrow-band k-distributions (or, in this case, C-distributions), which in turn need only be determined once for each ϕ and narrow band. This is the main objective of the present study, viz., to develop easy-to-access look-up tables of C-distributions that are conveniently set-up for being applied in the framework of the banded SLW model. The development of such tables, and how they can be used to assemble the partial ALBDF, are described in the next section.

3. NARROW-BAND C-DISTRIBUTIONS IN THE FRAMEWORK OF THE SLW MODEL

The narrow-band k-distribution model is based on the observation that, over a sufficiently narrow spectral interval, the highly oscillating absorption coefficient κ_η has the same value many times at slightly different wavenumbers. At each one of such occurrences, the resulting spectral radiative intensity and other radiative quantities will be approximately equal to each other (since, within a narrow interval, the spectral blackbody intensity can be regarded as constant). Therefore, k-distribution models propose a reordering of the absorption coefficient into a smooth, monotonically increasing function, whose integration over the narrow band is straightforward and can be carry out in a computationally efficient manner.

This idea of reordering the absorption coefficient dates back to the first half of the twentieth century (Kondratyev, 1969), and the first works on the subject in the heat transfer area were reported by Rivière *et al.*, 1992, 1994. In the present paper, we will focus only on the concept of the narrow-band k-distributions and on how they can be used to obtain the ALBDF and partial ALBDFs introduced in Sections 2.1 and 2.2. Thus, other aspects of the narrow-band k-distribution model, such as the treatment of gas mixtures and non-homogeneous media is not discussed here; the interested reader is referred to the books by Modest, 2013, and Howell *et al.*, 2016, for detailed presentations on these topics.

3.1 k- and C-distributions

The k-distribution is defined for a narrow band of width $\Delta\eta$ as (Modest, 2013)

$$f(k) = \frac{1}{\Delta\eta}\sum_i \left|\frac{\mathrm{d}\eta}{\mathrm{d}\kappa_\eta}\right|_i = \frac{1}{\Delta\eta}\int_{\Delta\eta} \delta(k-\kappa_\eta)\,\mathrm{d}\eta\,, \tag{7}$$

where $\delta(x)$ is the Dirac-delta function. Because, even across a very small $\Delta\eta$, $f(k)$ can display a quite erratic behavior (since $f(k)\to\infty$ whenever κ_η has a local minimum or maximum) it is convenient to introduce a cumulative k-distribution function $g(k) = \int_0^k f(k')\,\mathrm{d}k'$. For any given k value, this function represents the fraction of the spectrum for which the spectral absorption coefficient lies below k, and is thus bounded $0 \le g \le 1$. The inverse function $k(g)$ is smooth and monotonically increasing, with minimum and maximum values identical to those of the spectral absorption coefficient within the $\Delta\eta$ interval, and it is the basis of the narrow-band k-distribution model.

For the purpose of applying it for the calculation of the partial ALBDFs, it is useful to express the cumulative function g in terms of a variable C, that is related to the spectral absorption cross-section C_η the same way as k is related to κ_η. This ultimately leads to the following expression for $g(C,\phi)$:

$$g(C,\phi) = \frac{1}{\Delta\eta}\int_{\Delta\eta} H\big[C - C_\eta(\phi)\big]\,\mathrm{d}\eta\;; \tag{8}$$

notice that the dependence of both C_η (and, as a consequence, g) on the thermodynamic state ϕ is made explicit in this equation, similarly to Eqs. (4) and (6). The auxiliary variables C and k in the previous equations can be related via Eq. (3).

3.2 Assembling the ALBDF and partial-ALBDF from C-distributions

The assembly of the ALBDF, Eq. (4), from the narrow-band cumulative C-distribution functions, Eq. (8), can be carried out in a similar way as how full-spectrum k-distributions are calculated from narrow-band k-distributions (see, for instance, Modest and Riazzi, 2005). This ultimately leads to

$$F(C,\phi,T_b) = \sum_{i\in[\text{all NBs}]} \frac{I_{b,i}(T_b)}{I_b(T_b)}\, g_i(C,\phi), \tag{9}$$

where the summation takes place over all narrow bands, and $I_{b,i}(T_b) = \int_{\Delta\eta_i} I_{b\eta}(T_b)\,\mathrm{d}\eta$ is the spectral blackbody intensity integrated over narrow band i (and evaluated at the source temperature T_b). Similarly, the partial ALBDF for the spectral interval $\Delta\eta_m$ can be determined by restricting the summation in Eq. (9) to only the narrow bands that fall within η_{m-1} and

Table 1. Precalculated states for the narrow-band database

Parameter	Sampling	Number of samples
Species	CO_2, H_2O	2
CO_2 mole fraction	0.1	1
H_2O mole fraction	0, 0.1 and 0.2	3
Temperature [K]	300 to 2500: every 100	23
Narrow band [cm^{-1}]	10 to 300: every 10	29
	300 to 4000: every 25	148
	4000 to 5000: every 50	20
	5000 to 10 000: every 100	50
	10 000 to 15 000: every 250	20
	15 000 to 25 000: every 500	20
	Total	287

η_m:

$$F_{\Delta\eta_m}(C,\phi,T_b) = \sum_{\Delta\eta_i \in \Delta\eta_m} \frac{I_{b,i}(T_b)}{I_b(T_b)} g_i(C,\phi)\,. \tag{10}$$

Note that this formulation for determining the partial ALBDF differs slightly from the one presented by Modest and Riazzi, 2005, for the assembly of part-spectrum k-distributions in that, here, $F_{\Delta\eta_m}(C=0,\phi,T_b)=0$ for all $\Delta\eta_m$. This definition of $F_{\Delta\eta_m}$ is consistent with Eq. (6) and facilitates the application of the banded-SLW model.

4. GENERATION OF THE C-DISTRIBUTIONS

Data for the cumulative C-distribution g have been generated for carbon dioxide and water vapor for a total of 287 narrow bands. The position and size of the narrow bands are adapted from Cai and Modest, 2014, but both the number of bands and the total spectral range that they encompass have been expanded to now include the entire range of the CO_2 and H_2O absorption spectra; the narrow band sizes used here are also larger than those of Denison, 1994. The C-distributions are obtained at twenty-three temperatures, between 300 K and 2500 K; three mole fractions for H_2O, between 0 and 0.2; and one mole fraction for CO_2, 0.1 (considering only a single X for the latter species should suffice, given that its absorption spectrum does not present significant self-broadening effect (Howell *et al.*, 2016)). The total pressure is always kept at 1.0 atm. The discrete values and number of samples of each of these parameters are summarized in Table 1.

The nominal values for C used in Eq. (8) to construct the g database for each thermodynamic state and narrow band are determined using the exponential distribution previously employed by Wang and Modest, 2005. For the C variable, considering a narrow band and thermodynamic state where the minimum and maximum absorption cross-sections are C_{min} and C_{max}, respectively, this distribution gives

$$C_i = \left[(C_{min})^\beta + i\Delta(C^\beta)\right]^{1/\beta}; \qquad \Delta(C^\beta) = \frac{{C_{max}}^\beta - {C_{min}}^\beta}{N-1} \qquad (i=1,2,\ldots,N), \tag{11}$$

where N is the total number of C divisions in the narrow band, and β is a factor that controls how the C values are distributed (i.e., if they are more concentrated towards C_{min} or C_{max}). The distribution was found to require smaller N to produce accurate C-distributions than either a linear or a logarithmic distribution.

An important difference between the present C-distributions and the k-distributions proposed by Cai and Modest, 2014, and Wang and Modest, 2005, is that, while in those papers N and β were fixed (to 5000 and 0.1, respectively) for all narrow bands and thermodynamic states, here these restrictions are not applied. Rather, at each $\Delta\eta_i$ and each discrete ϕ, N is chosen as the smallest one whose errors in the band-averaged absorption coefficient and emittance are below 0.1 %; β, on the other hand, is defined as the value that provides (as best as possible) a g distribution with a distinct g-value g_i for each C_i. The advantage of this methodology is that it can produce C-distributions with the same accuracy that was reported for the k-distributions of Cai and Modest, 2014, and Wang and Modest, 2005, but the resulting data files are much smaller in size. For comparison, while in the databases of the aforementioned references each and every narrow band had a total of 5000 g_i values associated to it, in the databases generated in this paper the average value of N (computed over all narrow bands and thermodynamic states) is approximately 100.

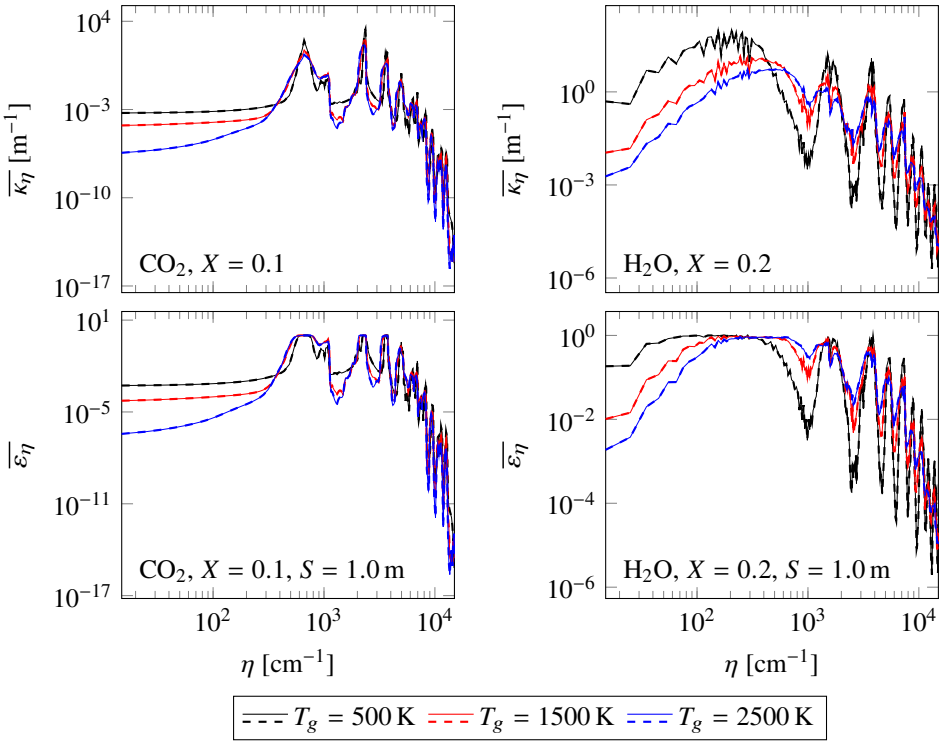

Figure 1. Comparisons of band-averaged absorption coefficient and emittance. Dashed lines represent the reference, LBL solution; solid thin lines depict the quantities recreated from the narrow-band C-distributions.

4.1 Base spectral data

The spectral data for the absorption cross-section C_η used to generate the C-distributions are obtained from the high-resolution spectroscopic database HITEMP2010 Rothman *et al.* (2010). The absorption spectra are extracted at a fixed 0.01 cm^{-1} wavenumber resolution and within a range $0 < \eta \leq 25\,000\,\text{cm}^{-1}$. Line broadening is described by the Lorentz profile, with line-wing cutoffs of 3000 half widths for the H_2O spectra and 30 000 half widths for the CO_2 ones, which are chosen following analyses carried out in a previous work (Coelho *et al.*, 2021).

4.2 Validation

The accuracy of narrow-band k-distributions has traditionally been assessed through comparisons of band-averaged absorption coefficient and gas column emittance (Wang and Modest, 2005; Cai and Modest, 2014). For a narrow band of width $\Delta\eta$, these quantities are given respectively as:

$$\overline{\kappa_\eta} = \frac{1}{\Delta\eta}\int_{\Delta\eta} \kappa_\eta \,\mathrm{d}\eta = \int_0^1 k(g)\,\mathrm{d}g \;; \tag{12}$$

$$\overline{\varepsilon_\eta} = \frac{1}{\Delta\eta}\int_{\Delta\eta} \left[1 - \exp\left(-\kappa_\eta S\right)\right] \mathrm{d}\eta = \int_0^1 \left[1 - \exp(-k(g)S)\right] \mathrm{d}g \;, \tag{13}$$

where S is the gas column width and $k(g)$ is the inverse function of the cumulative k-distribution $g(k)$ (notice that, once again, both κ_η and $k(g)$ can be related to C_η and $C(g)$ through Eq. (3)). Figure 1 plots the results for these two quantities obtained via LBL integration of the high-resolution absorption spectra—which corresponds to the expressions to the right-hand side of the first equal sign in Eqs. (12) and (13)—and recreated from the narrow-band C-distributions—the expressions after the last equal sign in the above equations—for pure CO_2 and pure H_2O and gas temperatures T_g of 500 K, 1500 K and 2500 K. The agreement between the two solution is excellent throughout the spectrum and for all thermodynamic conditions-. This is to be expected, since, as stated before, the C-distributions developed on this work were generated with the constraint that the maximum error relative to the LBL integration be less that 0.1 % for both $\overline{\kappa_\eta}$ and $\overline{\varepsilon_\eta}$. Similar accuracy was observed for other species mole fractions, temperatures and S values.

The ALBDF assembled from the narrow-band C-distributions via Eq. (9) is compared to the one determined directly from the high-resolution absorption spectra in Fig. 2. Plots for CO_2 and H_2O are presented considering source temperatures T_b = 500 K and 2500 K and gas temperatures (which, together with the species mole fraction, characterize

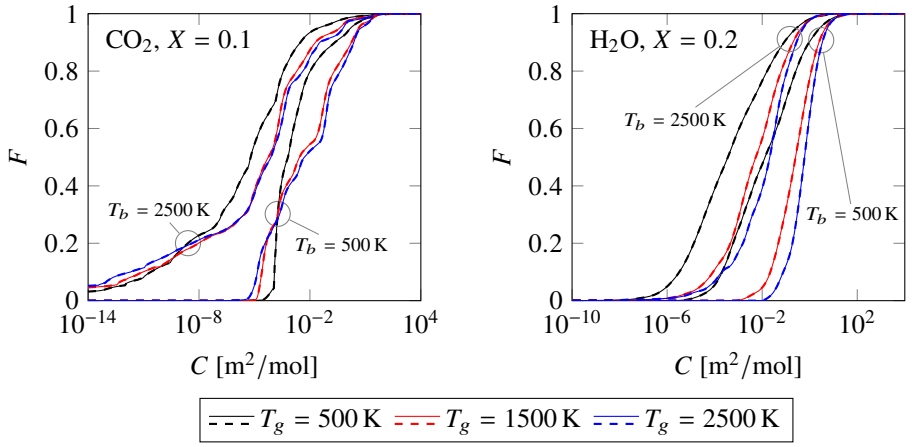

Figure 2. Comparisons of the ALBDF assembled from the narrow-band C-distributions (solid lines) and determined directly from the high-resolution spectra (dashed lines). Results for different source and gas temperatures T_b and T_g.

the thermodynamic state) $T_g = 500\,\text{K}$, 1500 K and 2500 K. The assembled ALBDF agrees very well with the reference throughout all the C range—to contrast, note that in a similar comparison, the narrow-band k-distributions of Modest and Riazzi, 2005 had some difficult to accurately construct full-spectrum k-distributions for very small k (which in Fig. 2 would correspond to very small C). The same degree of agreement between the two ALBDFs was verified for other source temperatures and thermodynamic states.

5. APPLICATION OF THE BANDED-SLW MODEL

A sample of test cases are now considered to illustrate the usefulness of the C-distributions produced in this paper. These cases all consist of non-coupled radiative transfer calculations of a one-dimensional medium slab of width $L = 1.0\,\text{m}$ bounded by two infinitely large, parallel, cold walls. The medium consists of a mixture of CO_2, H_2O and a transparent species at a total pressure of 1 atm, and is subjected to prescribed non-homogeneous fields of temperature and species mole fractions.

The radiative transfer calculations are carried out with either the SLW or the banded-SLW model and with the LBL integration method, which serves as a reference to assess the performance of the models. The same absorption spectra used to generate the C-distributions is employed for the LBL integration. The application of the SLW and banded-SLW models follow what is described in Sections 2.1 and 2.2, respectively. A total of $J = 25$ gases is chosen for both models (and, in the BSLW model, for each band as well), within a range $3 \times 10^{-4}\,\text{m}^2/\text{mol} \leq C \leq 60\,\text{m}^2/\text{mol}$. The treatment of mixtures of participating species is done according to the multiplication method (Solovjov and Webb, 2000), and non-homogeneous conditions are considered using the reference approach (Denison and Webb, 1995).

The angular integration of the RTE is performed through the discrete ordinates method (DOM), using the quadrature and weights of Lathrop and Carlson, 1964, with a total of twelve ordinates. A finite difference approach is applied to solve the RTE along each line of sight, which is divided into 200 equally-sized cells. Further increasing the angular and spatial discretizations did not yield appreciable changes in the results.

5.1 Case 1: the effect of the number of bands on the BSLW model's accuracy

The first test case considers that the medium is bounded by black walls. Since this case does not have non-gray wall reflectivities nor non-gray particulate, the standard, full-spectrum SLW model should suffice for this case; however, the BSLW is applied to it anyway to show how the division of the spectrum into bands improves the model's accuracy. The participating medium is subjected to the following non-isothermal temperature and non-uniform species mole fraction distributions:

$$T(x) = 400\,\text{K} + 1400\,\text{K}\sin^2\left(\pi\frac{x}{L}\right); \tag{14a}$$

$$X_c(x) = 0.1\sin^2\left(\pi\frac{x}{L}\right); \qquad X_w(x) = 2X_c(x), \tag{14b}$$

where X_c and X_w are the mole fractions of CO_2 and H_2O, respectively, and x is the distance within the medium measured from the left wall. Notice that $X_c(x) + X_w(x) < 1.0$, and the remainder of the medium is assumed to be composed of a non-participating species.

Figure 3 plots the resulting spatial distributions for the radiative heat source and radiative heat flux obtained by the LBL solution, the full-spectrum SLW model, and the BSLW model applied over a different total number of band divisions

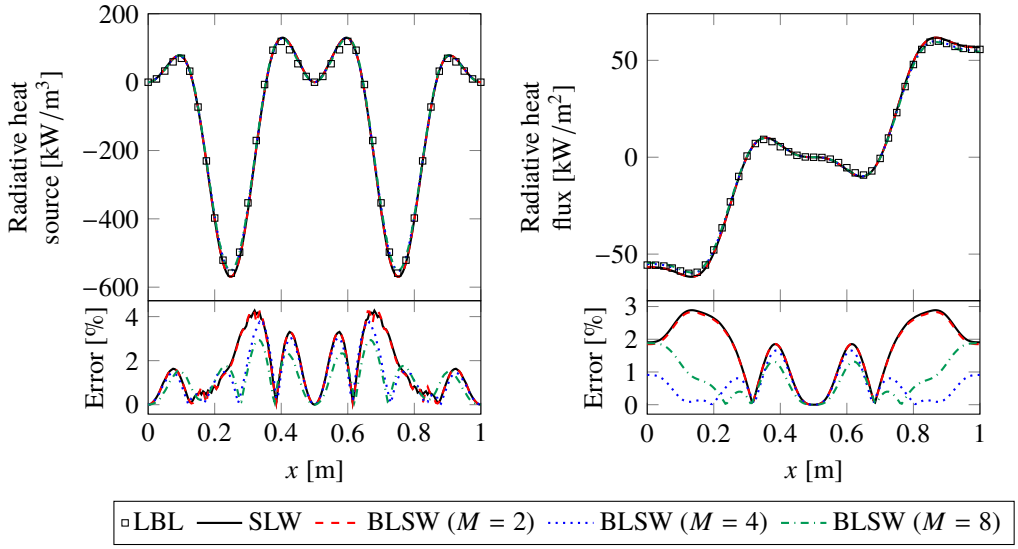

Figure 3. Results for test case 1.

M. Both the SLW and BSLW models use the ALBDF and partial-ALBDFs determined from the same absorption spectra for which the LBL calculations were ran (with the partial-ALBDFs determined from the narrow-band C-distributions via Eq. (10)). A uniform division of the entire spectral range $0 < \eta \leq 25\,000\,\mathrm{cm}^{-1}$ is adopted to define the size and position of the bands in the BSLW model—e.g., with $M = 2$, the first band spans from $\eta = 0$ to $\eta = 12\,500\,\mathrm{cm}^{-1}$, and the second band from $\eta = 12\,500\,\mathrm{cm}^{-1}$ to $\eta = 25\,000\,\mathrm{cm}^{-1}$. This spectral division is chosen out of convenience for this illustrative application of the model; certainly, more refined schemes could be devised, taking into account the local spectral maxima of C_η, which would further improve the accuracy of the BSLW model.

Although even the full-spectrum SLW model yields a very good agreement to the reference LBL solution, the BSLW model still provides a slight improvement. The bottom plots of Fig. 3 show the errors of SLW and BSLW models (normalized by the maximum radiative heat source and flux), from which it is clear that the latter, particularly with four or eight bands, outperforms the former. On average across the medium, the normalized error of the SLW model equals 1.7 % for both the radiative heat source and radiative heat flux, and locally the error can be as high as 4.3 %; for the BSLW model with $M = 8$, the average errors reduce to 1.1 % for the radiative heat source and 0.8 % for the radiative hear flux, and the maximum error is no higher than 3.0 %.

5.2 Case 2: a medium bounded by non-gray walls

A second test case is included to test the BSLW model for a medium bounded by non-gray walls, a configuration for which the standard SLW model cannot be applied. Here, the two walls exhibit the same spectral emissivity ϵ_η, characterized by the stepwise profile previously considered by Solovjov *et al.*, 2013, in which ϵ_η has three plateaus: $\epsilon_\eta = 0.925$ for $\eta \leq 2000\,\mathrm{cm}^{-1}$, $\epsilon_\eta = 0.675$ for $2000\,\mathrm{cm}^{-1} < \eta \leq 2500\,\mathrm{cm}^{-1}$, and $\epsilon_\eta = 0.500$ for $\eta > 2500\,\mathrm{cm}^{-1}$. The temperature and species concentration profiles are the same as those of Case 1.

For the BSLW model, the bands are chosen to coincide with the spectral intervals of constant ϵ_η, so that the radiative transfer problem can be reduced to three successive calculations of a medium bounded by gray walls. The resulting distributions for the radiative heat source and flux are depicted in Fig. 4. Besides the BSLW model and the reference LBL solution, the figure also include results obtained by applying the separated wall bands (SWB) method of Fonseca *et al.*, 2018, to the full-spectrum SLW model, which is another approach for accommodating for non-gray walls in the framework of global models. Notice that the computational costs of the SWB-SLW and BSLW models are approximately the same.

Figure 4 shows that the two models have comparable accuracy, with normalized errors (given by the bottom plots of the figure) not exceeding 6.0 %. In the high-emitting regions, the SWB-SLW tends to outperfom the BSLW, while the opposite occurs in the regions where absorption is more important. Similar results have been observed for other temperature, species concentrations and wall emissivity profiles.

6. CONCLUSIONS

This paper presented the development of narrow-band C-distributions for water vapor and carbon dioxide encompassing a range of thermodynamic conditions that is common for combustion applications. These distributions were generated from high-resolution absorption spectra and, compared to narrow-band k-distributions that are available in the literature, they are set up in a more convenient way for being used with the SLW and banded-SLW models.

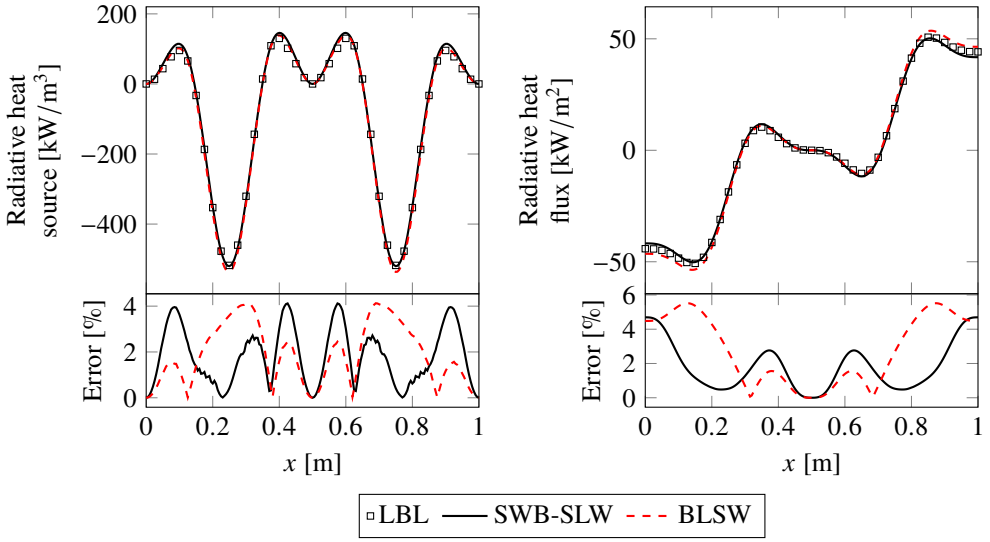

Figure 4. Results for test case 2.

The new C-distributions were shown to yield an excellent agreement with reference data computed directly from the high-resolution spectrum for band-averaged quantities across all the considered thermodynamic states. The same was also verified for the assembled ALBDFs. Furthermore, besides having comparable accuracy to previous k-distributions, the C-distributions proposed here require a significantly smaller storage size. Interested readers can get access to the data sets with these distributions by contacting the first author of this paper.

Finally, the C-distributions were used to construct partial ALBDFs for the banded-SLW model, and the model was applied to a few illustrative cases. In the first one, it was shown that, by dividing the full spectrum into bands, the BSLW model can consistently improve on the already good accuracy of the standard SLW model. In the second case, the capacity of the BSLW model to accommodate for non-gray walls was assessed, and the model was found to yield similar accuracy (and similar computational cost) as a previous modeling approach for treating non-gray walls with the SLW model.

7. ACKNOWLEDGMENTS

Author GCF thanks the National Council for Scientific and Technological Development (CNPq) for a postdoctoral scholarship. This study was financed in part by the Coordenação de Aperfeiçoamento de Pessoal de Nível Superior - Brasil (CAPES) - Finance Code 001.

8. REFERENCES

Cai, J. and Modest, M.F., 2014. "Improved full-spectrum k-distribution implementation for inhomogeneous media using a narrow-band database". *Journal of Quantitative Spectroscopy and Radiative Transfer*, Vol. 141, pp. 65–72. doi:10.1016/j.jqsrt.2014.02.028.

Coelho, F.R., Ziemniczak, A., Roy, S.P. and França, F.H., 2021. "A new line-by-line methodology based on the spectral contributions of the bands". *International Journal of Heat and Mass Transfer*, Vol. 164, p. 120423. doi:10.1016/j.ijheatmasstransfer.2020.120423.

Denison, M.K., 1994. *A spectral line-based weighted-sum-of-gray-gases model for arbitrary RTE solvers*. Ph.D. thesis, Brigham Young University, Provo, Utah.

Denison, M.K. and Webb, B.W., 1995. "The spectral line-based weighted-sum-of-gray-gases model in nonisothermal nonhomogeneous media". *Journal of Heat Transfer*, Vol. 117, No. 2, pp. 359–365. doi:10.1115/1.2822530.

Denison, M.K. and Webb, B.W., 1993a. "An absorption-line blackbody distribution function for efficient calculation of total gas radiative transfer". *Journal of Quantitative Spectroscopy and Radiative Transfer*, Vol. 50, No. 5, pp. 499–510. doi:10.1016/0022-4073(93)90043-h.

Denison, M.K. and Webb, B.W., 1993b. "A spectral line-based weighted-sum-of-gray-gases model for arbitrary RTE solvers". *Journal of Heat Transfer*, Vol. 115, No. 4, pp. 1004–1012. doi:10.1115/1.2911354.

Denison, M.K. and Webb, B.W., 1994. "k-distributions and weighted-sum-of-gray-gases–a hybrid model". In *Proceedings of the International Heat Transfer Conference 10*. Begellhouse. doi:10.1615/ihtc10.4890.

Fonseca, R.J.C., Fraga, G.C., da Silva, R.B. and França, F.H.R., 2018. "Application of the WSGG model to solve the radiative transfer in gaseous systems with nongray boundaries". *Journal of Heat Transfer*, Vol. 140, No. 5, p. 052701. doi:10.1115/1.4038548.

Goody, R.M. and Yung, Y.L., 1995. *Atmospheric Radiation: Theoretical Basis*. Oxford University Press, 2nd edition.

Howell, J.R., Mengüç, M.P. and Siegel, R., 2016. *Thermal Radiation Heat Transfer*. CRC press, 6th edition.

Kondratyev, K.Y., 1969. *Radiation in the Atmosphere*. Academic Press, New York, USA.

Lacis, A.A. and Oinas, V., 1991. "A description of the correlated-k distribution method for modeling nongray gaseous absorption, thermal emission, and multiple scattering in vertically inhomogeneous atmospheres". *Journal of Geophysical Research*, Vol. 96, No. D5, p. 9027. doi:10.1029/90jd01945.

Lathrop, K.D. and Carlson, B.G., 1964. "Discrete ordinates angular quadrature of the neutron transport equation". Technical report, Los Alamos Scientific Laboratory of the University of California, Los Alamos, New Mexico, USA. doi:10.2172/4666281.

Modest, M.F., 1991. "The weighted-sum-of-gray-gases model for arbitrary solution methods in radiative transfer". *Journal of heat transfer*, Vol. 113, No. 3, pp. 650–656. doi:10.1115/1.2910614.

Modest, M.F., 2013. *Radiative Heat Transfer*. Academic Press.

Modest, M.F. and Riazzi, R.J., 2005. "Assembly of full-spectrum k-distributions from a narrow-band database; effects of mixing gases, gases and nongray absorbing particles, and mixtures with nongray scatterers in nongray enclosures". *Journal of Quantitative Spectroscopy and Radiative Transfer*, Vol. 90, No. 2, pp. 169–189. doi:10.1016/j.jqsrt.2004.03.007.

Modest, M.F. and Zhang, H., 2002. "The full-spectrum correlated-k distribution for thermal radiation from molecular gas-particulate mixtures". *Journal of heat transfer*, Vol. 124, No. 1, pp. 30–38. doi:10.1115/1.1418697.

Ozen, G., Ates, C., Selçuk, N. and Kulah, G., 2019. "Assessment of SLW-1 model in the presence of gray and non-gray particles". *International Journal of Thermal Sciences*, Vol. 136, pp. 420–432. doi:10.1016/j.ijthermalsci.2018.10.038.

Pearson, J.T., Webb, B.W., Solovjov, V.P. and Ma, J., 2014. "Efficient representation of the absorption line blackbody distribution function for h2o, CO2, and CO at variable temperature, mole fraction, and total pressure". *Journal of Quantitative Spectroscopy and Radiative Transfer*, Vol. 138, pp. 82–96. doi:10.1016/j.jqsrt.2014.01.019.

Rivière, P., Soufiani, A. and Taine, J., 1992. "Correlated-k and fictitious gas methods for H_2O near 2.7 μm". *Journal of Quantitative Spectroscopy and Radiative Transfer*, Vol. 48, No. 2, pp. 187–203. doi:10.1016/0022-4073(92)90088-l.

Rivière, P., Scutaru, D., Soufiani, A. and Taine, J., 1994. "A new ck data base suitable from 300 to 2500 K for spectrally correlated radiative transfer in CO_2-H_2O-transparent gas mixtures". In *Proceeding of International Heat Transfer Conference 10*. Begellhouse. doi:10.1615/ihtc10.5070.

Rothman, L.S., Gordon, I.E., Barber, R.J., Dothe, H., Gamache, R.R., Goldman, A., Perevalov, V.I., Tashkun, S.A. and Tennyson, J., 2010. "HITEMP, the high-temperature molecular spectroscopic database". *Journal of Quantitative Spectroscopy and Radiative Transfer*, Vol. 111, No. 15, pp. 2139–2150. doi:10.1016/j.jqsrt.2010.05.001.

Solovjov, V.P., Lemonnier, D. and Webb, B.W., 2013. "Efficient cumulative wavenumber model of radiative transfer in gaseous media bounded by non-gray walls". *Journal of Quantitative Spectroscopy and Radiative Transfer*, Vol. 128, pp. 2–9. doi:10.1016/j.jqsrt.2012.07.017.

Solovjov, V.P. and Webb, B.W., 2000. "An efficient method for modeling radiative transfer in multicomponent gas mixtures with soot". *Journal of Heat Transfer*, Vol. 123, No. 3, pp. 450–457. doi:10.1115/1.1350824.

Solovjov, V.P., Webb, B.W. and Andre, F., 2018. "Radiative properties of gases". In *Handbook of Thermal Science and Engineering*, Springer International Publishing, pp. 1069–1141. doi:10.1007/978-3-319-26695-4_59.

Wang, A. and Modest, M.F., 2005. "High-accuracy, compact database of narrow-band k-distributions for water vapor and carbon dioxide". *Journal of Quantitative Spectroscopy and Radiative Transfer*, Vol. 93, No. 1-3, pp. 245–261. doi:10.1016/j.jqsrt.2004.08.024.

Webb, B.W., Solovjov, V.P. and André, F., 2019. "The spectral line weighted-sum-of-gray-gases (SLW) model for prediction of radiative transfer in molecular gases". In *Advances in Heat Transfer*, Elsevier, pp. 207–298. doi:10.1016/bs.aiht.2019.08.003.

Yasar, M.S., Ozen, G., Selçuk, N. and Kulah, G., 2020a. "Assessment of improved banded model for spectral thermal radiation in presence of non-gray particles in fluidized bed combustors". *Applied Thermal Engineering*, Vol. 176, p. 115322. doi:10.1016/j.applthermaleng.2020.115322.

Yasar, M.S., Ozen, G., Selçuk, N. and Kulah, G., 2020b. "Performance of banded SLW-1 in presence of non-gray walls and particles in fluidized bed combustors". *Journal of Quantitative Spectroscopy and Radiative Transfer*, Vol. 257, p. 107370. doi:10.1016/j.jqsrt.2020.107370.

Yasar, M.S., Selçuk, N. and Kulah, G., 2021a. "Influence of bag filter ash to spectral thermal radiation in fluidized bed combustors co-fired with biomass". *International Journal of Thermal Sciences*, Vol. 167, p. 107012. doi:10.1016/j.ijthermalsci.2021.107012.

Yasar, M.S., Selçuk, N. and Kulah, G., 2021b. "Influence of soot on radiative heat transfer in bubbling fluidized bed combustors". *Journal of Quantitative Spectroscopy and Radiative Transfer*, Vol. 270, p. 107711. doi:10.1016/j.jqsrt.2021.107711.

9. RESPONSIBILITY NOTICE

The authors are solely responsible for the printed material included in this paper.